New insights into seismic behavior of building and surrounding soil at Hamaoka nuclear power station during Suruga Bay earthquake in 2009

S. Kamagata[1] and I. Takewaki*[2]

[1] *Nuclear Power Department, Kajima Corporation, Tokyo 107-8348, Japan*

[2] *Dept of Architecture and Architectural Eng., Kyoto University, Kyoto 615-8540, Japan*

**Corresponding author: takewaki@archi.kyoto-u.ac.jp*

Abstract. The Suruga Bay earthquake in 2009 attacked the Hamaoka nuclear power station and stopped the operation. The maximum acceleration 4.38m/s^2 at the foundation of the reactor building of No.5 unit was four times larger than that of No.1 unit. It was found that the vibration amplitude at 2.5Hz is mainly related to that maximum acceleration. The records in the underground support the fact that the vibration amplification was caused in the surface soil from 25 to 100 meters beneath the reactor building. The non-stationary Fourier spectra clarified that the frequency of the dominant component shifted from 3.0Hz to 2.5Hz in the short transient time. The dual-peak shape in the displacement profile was assumed to consist of the fundamental mode and the local vibration mode and this was identified by the dual Ricker wavelets. This identification indicates that the vibration amplification was caused by the deformation with the amplitude of 20mm in the underground. The average strain of soil from SRϕ-22 (22m underground) to SRϕ-100 (100m underground) reached 0.031% which reduced 30% of shear stiffness. The rocking mode of the foundation was further observed from the vertical deformation of the foundation. By investigating the phase of the displacement profile, it was found that the natural period at the north position was longer than that at the south position, which is related to the nonlinearity of the supporting soil.

Keywords: large acceleration, nuclear power plant station, soil-structure interaction, surface soil amplification, local vibration mode, rocking mode of foundation, non-stationary Fourier spectra, Ricker wavelet

1. Introduction

Many large ground accelerations have recently been observed near the nuclear power station (NPS) sites in Japan. In order to investigate the interaction between the building and its surrounding soil, several analytical researches have been conducted. For example, the maximum acceleration 6.80m/s^2 at the reactor building (No.1 unit) of Kashiwazaki-Kariwa NPS was recorded during the Niigata-ken Chuetsu-oki earthquake in 2007 and many researches were conducted [1]. It was found that the gap between the foundation and its contacting soil caused the amplified pulse wave in the acceleration record [2-4].

The Suruga Bay earthquake in 2009 (see Fig.1 [5]) attacked the Hamaoka NPS (see Fig.2(a) [6]) and the maximum acceleration 4.38m/s^2 was measured at the foundation of the reactor building (No.5 unit) [7]. The maximum acceleration at the No.5 unit was four times larger than that at the No.1 unit. In order to investigate the variance of the maximum accelerations at No.1 through No.5 unit, many researches were conducted including the geological field research. The Chubu Electric Power Company Co., Inc. conducted the research of the offset vertical seismic profile (VSP) using deep well boring and reported that the existence of the soft soil from 200m to 400m below the ground surface with the shear wave velocity (700 - 800m/s) 30-percent lower than that of the soil around that soil region is the main factor of the amplification based on the analytical results by the 2-dimentional finite difference method [8-11] (see Fig.2(b)). This is the opinion of Chubu Electric Power Co., Inc. Matsumoto [12] concluded that the property of the propagation process from the epicenter to the site was the main factor of the amplification and the property of the surrounding soil and the seismic fault had less effect on the amplification.

The seismic records measured by the Chubu Electric Power Company Co., Inc. were distributed from the Japan Association for Earthquake Engineering [13]. They included the seismic records at the surrounding soil of the reactor buildings. By using these records, the interaction between the soil and the building can be evaluated. Furthermore the seismic records of K-NET [14] can be analyzed to evaluate the seismic behavior of the Hamaoka area neighboring the Hamaoka NPS. It is shown that several vertical seismic records on the foundation are useful to evaluate the seismic behavior of the foundation, such as the uplift of foundations, which leads to the amplified seismic response.

The occurrence mechanism of the large acceleration has been a central issue in the seismic design of nuclear power plants and many investigations have been conducted [15-17]. The seismic behavior of the Kashiwazaki-Kariwa NPS during Niigata-ken Chuetsu-oki earthquake in 2007 was investigated from the seismic records at the surface ground level [4]. On the contrary, the seismic records at the Hamaoka NPS during the

Suruga Bay earthquake in 2009 included the seismic records in the underground which also enable the analysis of the actual seismic behavior in the surface soil. In order to evaluate the local vibration mode in the acceleration record, the non-stationary Fourier spectra [18] and the numerically integrated displacement profile are used (Appendix-1). The clarification of the unusual amplification in the surface soil and the rocking response of the foundation is the principal objective in this paper.

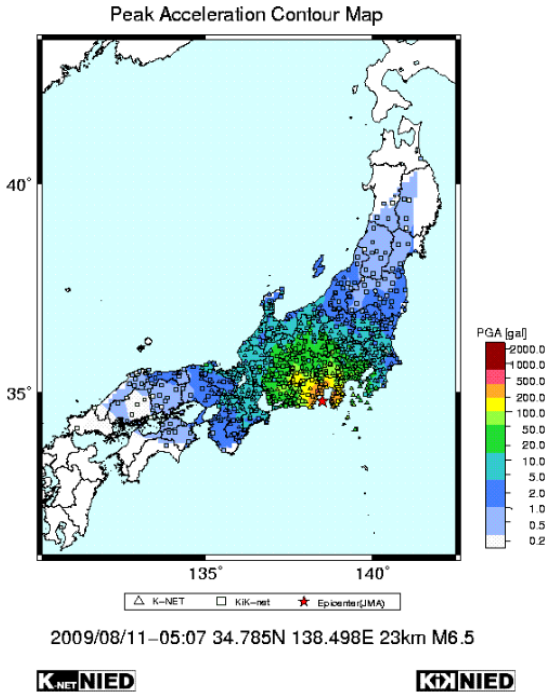

Fig.1 Suruga Bay earthquake in 2009 [5]

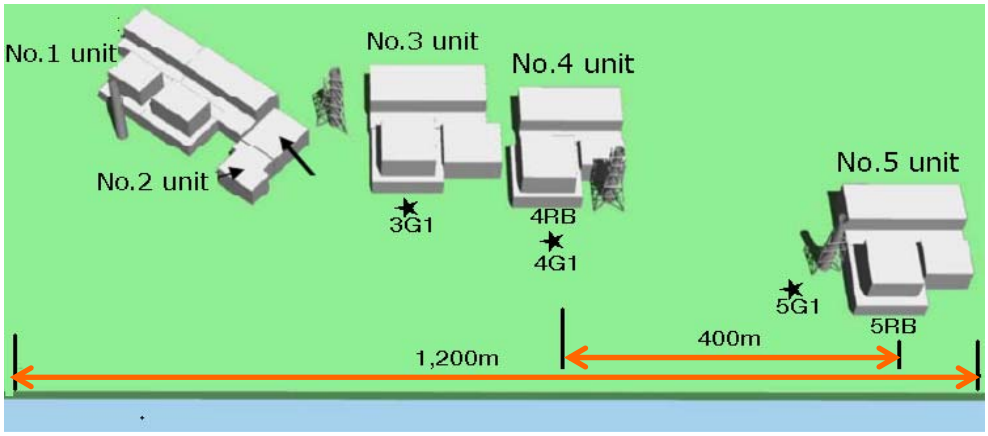

Fig.2(a) Site-map of Hamaoka NPS [6] and layout of nuclear power plant units

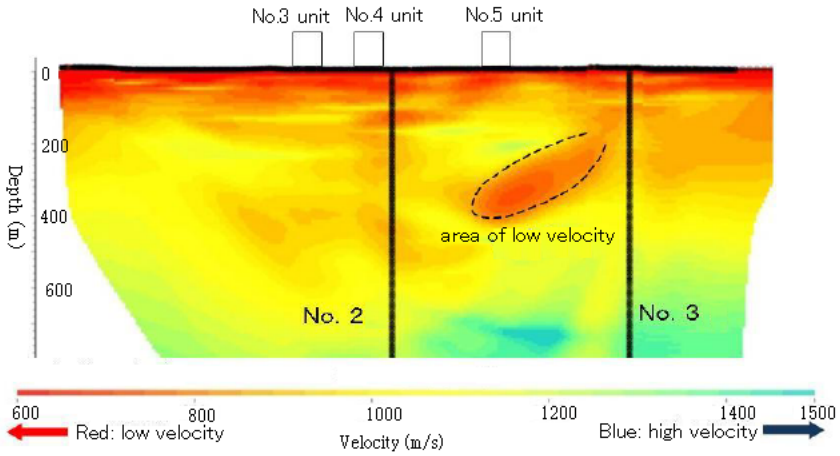

Fig.2(b) Deep ground profile
(http://www.chuden.co.jp/corporate/publicity/pub_release/press/__icsFiles/afieldfile/2011/02/25/12151.pdf (Accessed on June 3rd))

2. Amplification by local vibration mode of surface soil

At the Hamaoka NPS site, many seismometers are arranged as a high density seismic array system (see Fig.2(a)). Several seismometers are arranged on the foundation of the reactor building (RB) (see Fig.3). Their seismic records are useful to evaluate the seismic behavior of the foundation. Furthermore many seismometers are arranged in the underground beneath and around the reactor building and their seismic records are useful to evaluate the interaction between the soil and the reactor building.

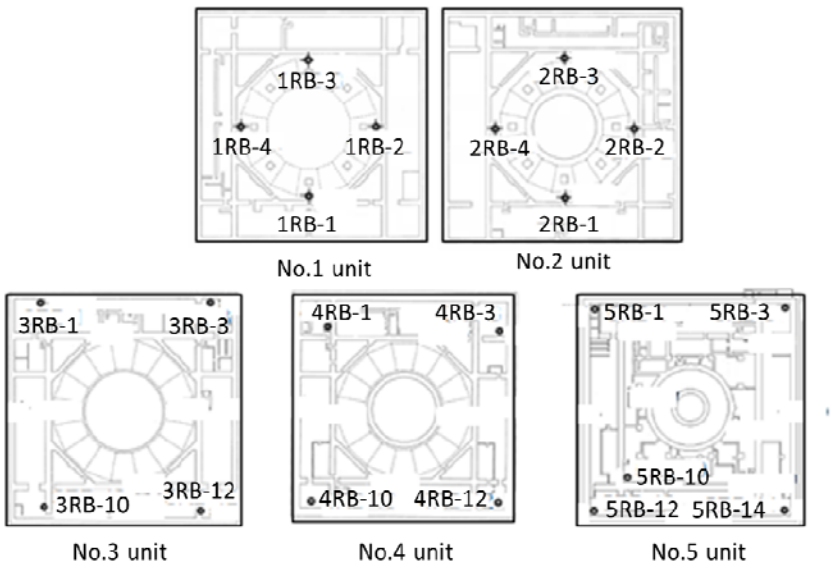

Fig.3 Arrangement of accelerometers in reactor buildings (RB: BF2-floor)

2.1 Seismic records on foundation from No.1 to No.5 unit

The arrangement of seismometers at the foundation from No.1 through No.5 unit is shown in Fig.3. Their maximum accelerations at the foundation are listed in Table 1 and those values are compared with the values at the K-NET (Hamaoka and Haibara) in Fig.4. The seismic records of the K-NET (Hamaoka and Haibara) are investigated in Appendix-2. As for the EW component, the maximum acceleration at the No.5 unit is four times larger than that at the No.1. The shear wave velocity at the Hamaoka NPS is around 700m/s (Fig.5). Fig.5 is illustrated based on the construction permission document for the Hamaoka nuclear power plant.

The acceleration profiles during 5-10 seconds including the main shock are illustrated in Fig.6. The phase and amplitude of the acceleration profile in each side-by-side units, such as No.1 and No.2 units, No.3 and No.4 units, resemble each other and those at the No.5 unit are different from those at other units. This may be related to the difference of the reactor type shown in Fig.7 and the position in the NPS site.

Especially the amplification at the No.5 unit has a peculiar characteristic between 6 and 7 seconds. The difference may be dependent on the wave propagation property from the epicenter to the Hamaoka site [10, 19].

Table 1 Maximum acceleration on BF2-floor of reactor building (m/s^2)

component	No.1 unit	No.2 unit	No.3 unit	No.4 unit	No.5 unit
NS	0.69	0.72	0.68	1.10	2.19
EW	1.10	1.10	1.46	1.78	4.39
UD	0.48	0.31	0.63	0.68	0.84

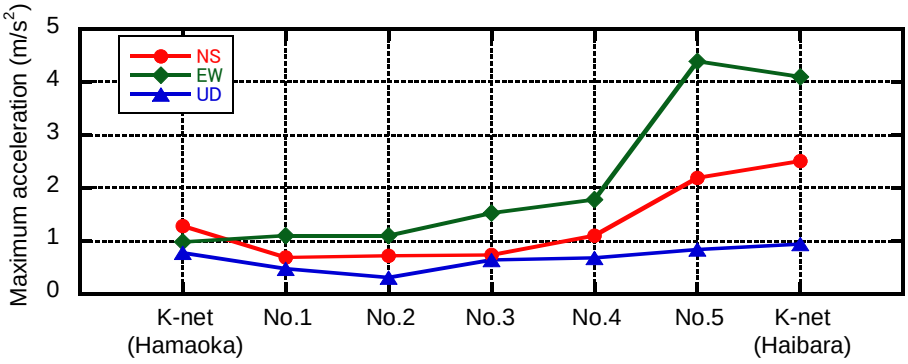

Fig.4 Maximum acceleration at BF2-floor of reactor building

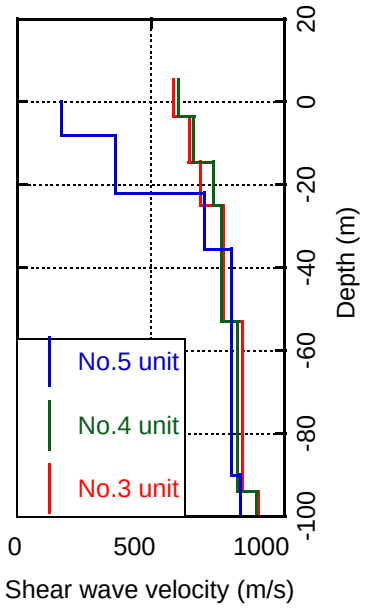

Fig.5 Shear wave velocity of soil at Hamaoka NPS

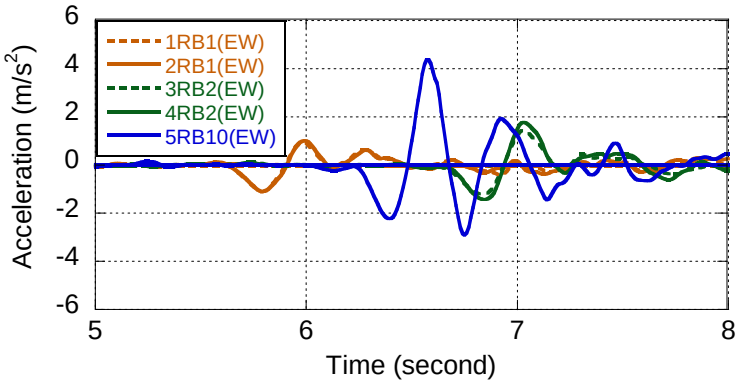

Fig.6 Acceleration profiles of EW component at No.1-5 units (BF2-floor)

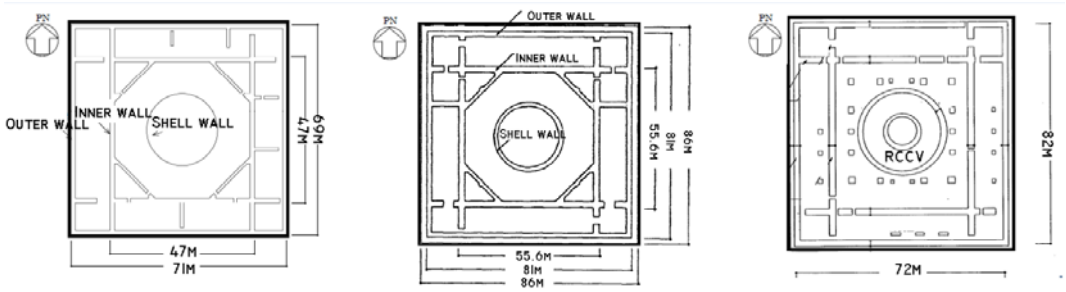

No.1 & 2 unit (Mark-2)　No.3 & 4 unit (Adv.Mark-2)　No.5 unit (ABWR)

Fig.7 Size and type of reactor building

2.2 Locality of amplification in depth direction

The amplification property at the No.5 unit was evaluated in the depth direction by using the seismic records measured beneath the reactor building (see Fig.8).

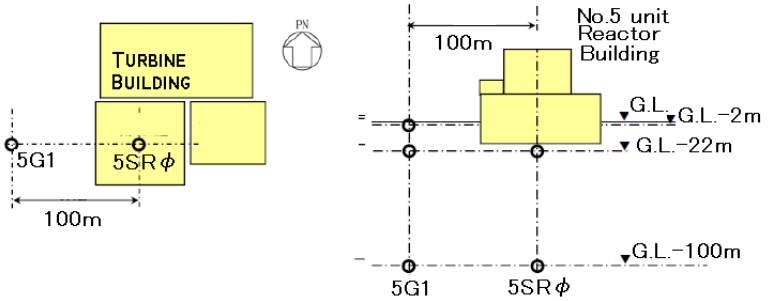

Ground plan Cross-section

Fig.8 Position of accelerometer in underground beneath No.5 unit

The non-stationary Fourier spectrum is illustrated as a contour with the horizontal axis of time (second) and the vertical axis of frequency (Hz). The maximum amplitudes are normalized by the maximum value of the Fourier amplitude and the value of percent is adopted in the figures.

$F(\omega_i; T_j)$; Non-stationary Fourier spectra at surface $(T_j;\ j = 1,2,\cdots M)$

F_{MAX} : Maximum value of $F(\omega_i; T_j)$

in frequency $(\omega_i; i = 1,2,\cdots N/2)$ and duration $(T_j;\ j = 1,2,\cdots M)$

$F_{Ratio}(\omega_i; T_j) = F(\omega_i; T_j)/F_{MAX}$:

$M = T/\Delta T$ T ; Duration of seismic record

ΔT ; Time interval of FFT analysis

N: Number of steps in FFT analysis

The non-stationary Fourier spectra of the seismic records beneath the reactor building (No.5 unit) and the maximum amplitude spectra are shown in Fig.9. The frequency of the maximum dominant component is 2.5Hz at 5RB10 (Reactor Building) and 5SRϕ-22 and is 3.0Hz at 5SRϕ-100. The maximum amplitude at 5SRϕ-22 is one and half times larger than that at 5SRϕ-100.

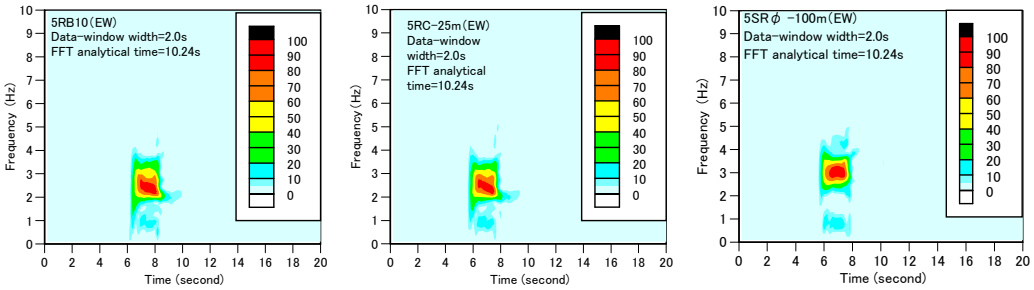

on foundation GL-22 meters GL-100 meters

No.5 unit foundation and underground (EW component)

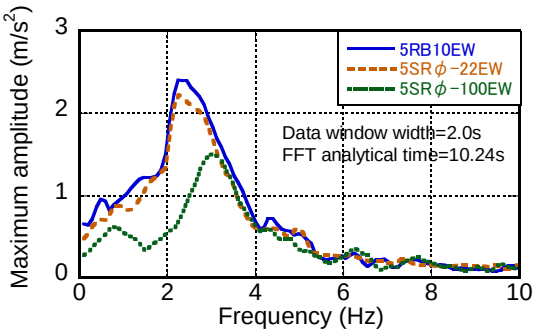

Fig.9 Non-stationary Fourier spectra (top) and maximum amplitude spectra (bottom) beneath the center of reactor building

To make clear the spread of the local amplification phenomenon in the depth direction, their displacement profiles are compared in Fig.10. The shape of dual peaks around 7 seconds is observed at 5RB10 and 5SRϕ-22. On the other hand, the displacement profile at 5SRϕ-100 (EW) shows the shape of a single peak. The difference of these peak shapes may result from the fact that the movement in the opposite direction occurred in the underground between 22 and 100 meters (see Fig.11).

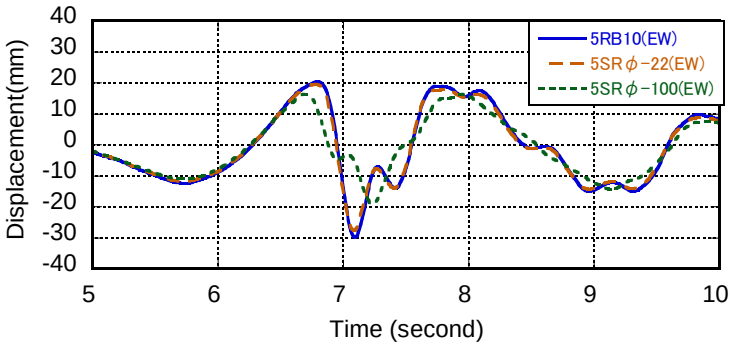

Fig.10 Displacement profile at various depths (No.5 unit)

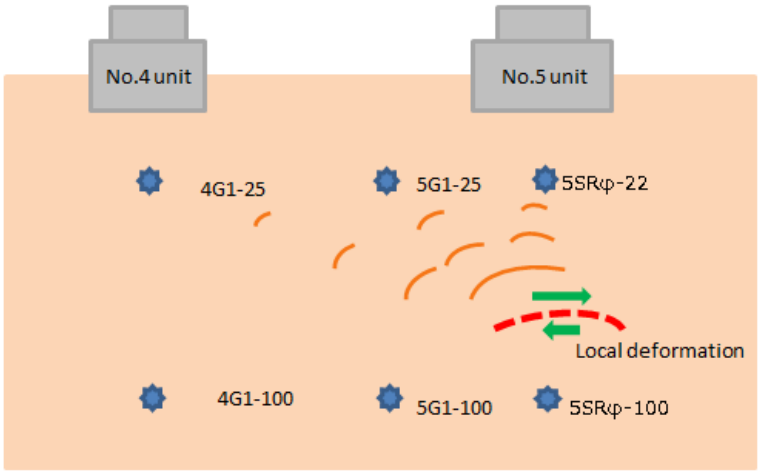

Fig.11 Assumed local deformation in underground

The soil shear strain time-histories are shown in Fig.12 (left). The maximum strain of the EW component is 0.031%. The strain was calculated by using the assumption of linear distribution from SRϕ-22 (22m underground) to SRϕ-100 (100m underground). This means that the local modes between two points were neglected. In the seismic design of the Hamaoka nuclear power station, the soil nonlinearity was evaluated by the G-γ relation as shown in Fig.12 (right). The stiffness reduction ratio (G/G_0) for the evaluated maximum strain is about 0.7.

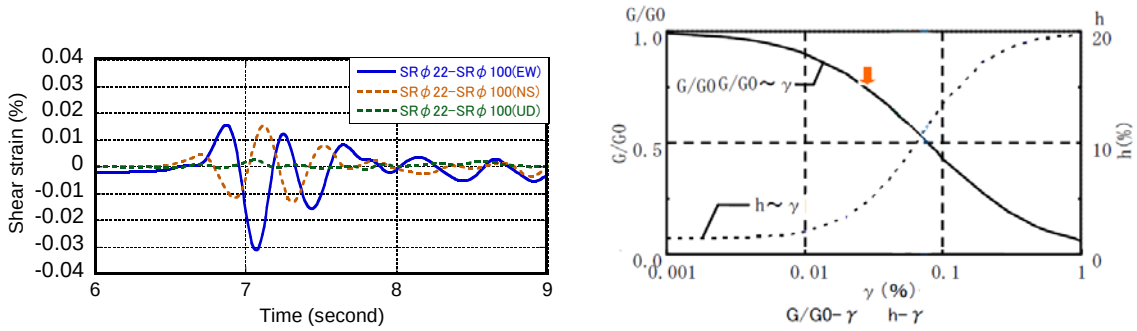

Fig.12 Soil strain time-histories and amplitude dependence of soil properties

2.3 Locality of amplification in horizontal direction

To evaluate the local amplification phenomenon in the horizontal direction, the seismic records at 5G1, 4G1, and 3G1 are analyzed (see Fig.13).

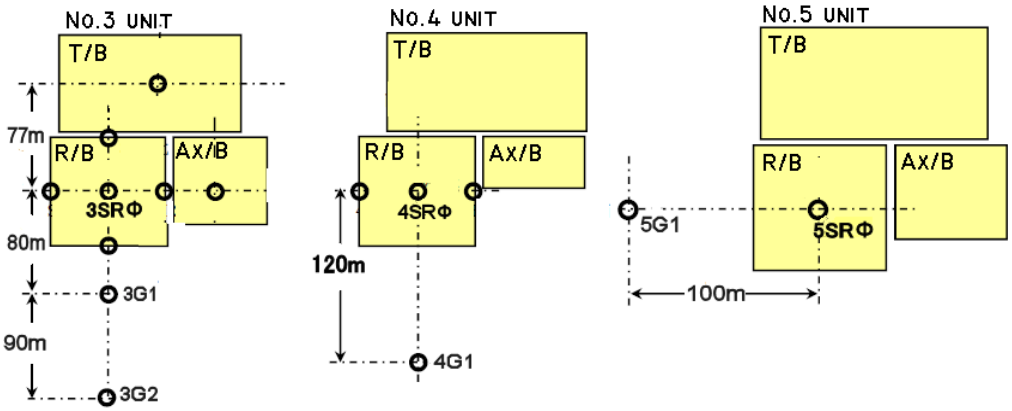

Fig.13 Position of accelerometer at No.3, 4 and 5 units [7]

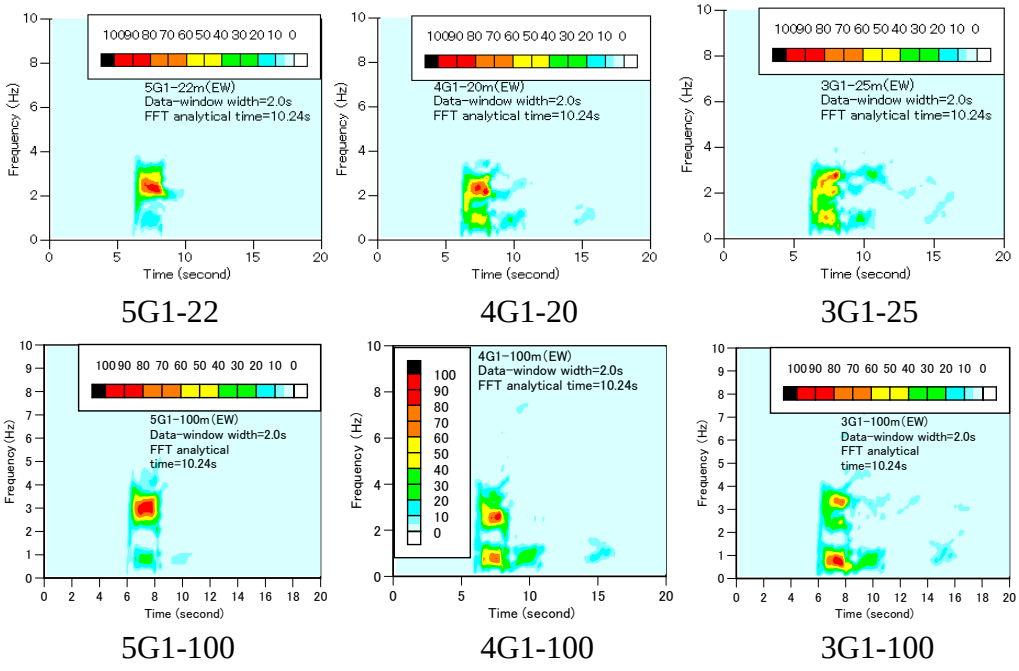

5G1-22 4G1-20 3G1-25

5G1-100 4G1-100 3G1-100

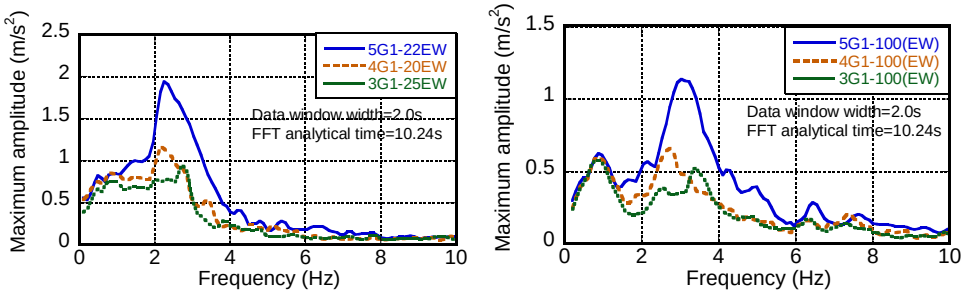

Underground (GL-25 meters) Underground (GL-100 meters)

Fig.14 Comparison of non-stationary Fourier spectra (top) and maximum amplitude spectra (bottom) in depth direction at No.3, No.4 and No.5 units

In order to evaluate the distribution property of the dominant component, the non-stationary Fourier spectra at 5G1, 4G1 and 3G1 and the maximum amplitude spectra are compared in Fig.14.

The frequency of the dominant component is 2.2Hz at 5G1-22m and 4G1-20m and 2.7Hz at 3G1-25m. The frequency at the No.5 unit is lower than that at No.3. Furthermore the frequency of the dominant component is 2.9Hz at 5G1-100m, 2.6Hz at 4G1-100m and 3.3Hz at 3G1-100m. The dominant frequency of the record at GL-100m is higher than that at GL- 22m.

The maximum amplitude is 1.93m/s at 5G1-22m, which is two times larger than the value 1.0m/s at 3G1-25m, and the value 1.14m/s at 5G1-100m is also two times larger than the value 0.53m/s at 3G1-100m. The value 0.6m/s at 0.8Hz is common in 5G1-100m, 4G1-100m and 3G1-100m, which is considered as the fundamental mode of the underground soil.

To make clear the seismic behavior of the local amplification at 5RB10 in the horizontal direction, the displacement profiles at No.3, No.4 and No.5 units are compared in the same figure at GL-20, 22, 25m and GL-100m beneath the reactor building (see Fig.15). The fundamental modes of three records are almost coincident and are related to the common component of 0.8Hz. The shape of dual peaks is only observed in the displacement profile at 5SRϕ-22 around 7 seconds. From these analytical results, we can conclude that the amplification at the No.5 unit is restricted around the No.5 unit.

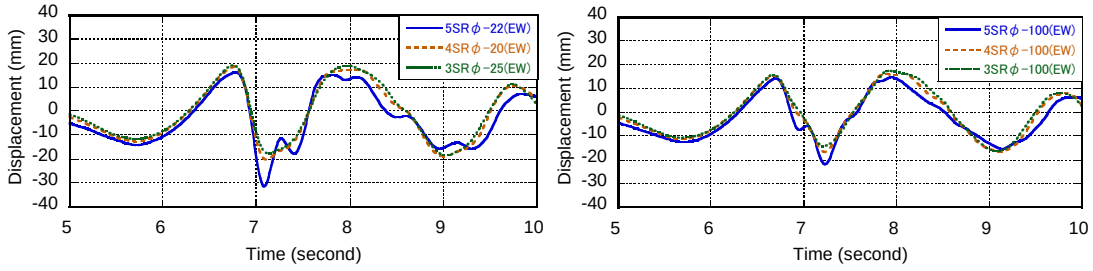

SRϕ-22 SRϕ-100

Fig.15 Comparison of displacement profiles at various depths (No.3-5 units)

The acceleration and displacement profiles at 5RB10 (EW) are illustrated in Fig.16. It can be observed that the maximum acceleration occurred in the process of the maximum peak-to peak displacement around 7 seconds.

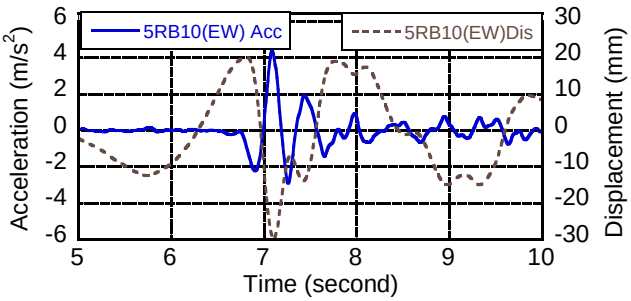

Fig.16 Relation of acceleration and displacement profiles at foundation of No.5 unit

2.4 Transient change of dominant frequency

By analyzing the seismic records, some special phenomena have been observed which may be caused by the nonlinearity in the supporting soil. In this section, the mechanism of amplification in the surface soil is investigated by using the non-stationary Fourier spectra with the frequency range lower than 5Hz.

From the non-stationary Fourier spectra at 5RB10(EW), it can be observed that the frequency of the dominant vibration component contributing to the maximum acceleration 4.38m/s^2 changes from 3.0Hz to 2.0Hz as the time passes from 6.5 to 8 seconds. This phenomenon is not observed in the non-stationary Fourier spectra at the No.4 unit. Therefore the amplification at the No.5 unit is considered to be caused by the local vibration mode with the amplitude 2.50m/s^2 (see Fig.17).

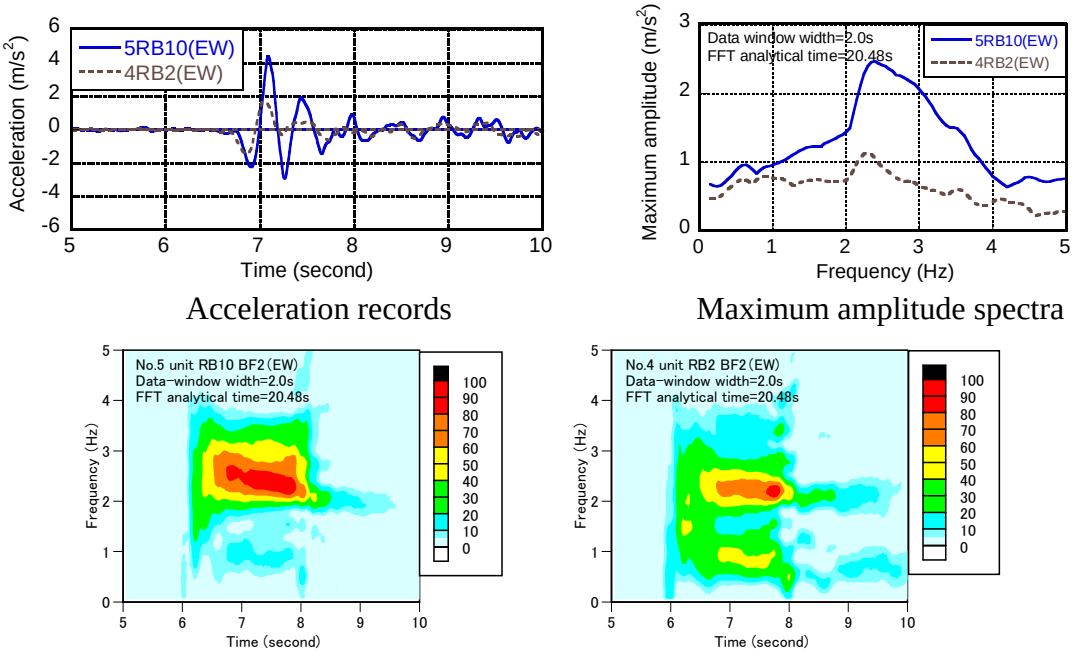

Acceleration records　　Maximum amplitude spectra

No.5 unit (RB10)　　No.4 unit (RB2)

Non-stationary Fourier spectra

Fig.17 Change of dominant frequency in terms of non-stationary Fourier spectra

2.5 Deformation profile of local mode at surface soil

The occurrence process of the dominant vibration component around 7 seconds is investigated by using the integrated displacement profile, as shown in Fig.18(a), at 5RB10, 5SRϕ-22and 5SRϕ-100. The deformation profiles of the underground soil are illustrated with the interval of 0.05 seconds using the data of G.L.-10m, G.L.-22m and G.L.-100m in Fig.18(b). In the interval from 6.8 to 7.1 seconds, the incremental displacement at 5SRϕ-22 and 5RB10 exceeds 10mm. In the time from 7.1 to 7.3 seconds and from 7.3 seconds to 7.4 seconds, the direction of movement at 5SRϕ-100 is opposite to the movement at 5Rϕ-22. The maximum acceleration 4.38m/s^2 at 5RB10 was caused in this local vibration mode. In the displacement profile at the No.4 unit, the phase at the 5SRϕ-22 corresponds with the phase at 5SRϕ-100 and dual peaks do not appear around 7 seconds (see Fig.19 (a)).

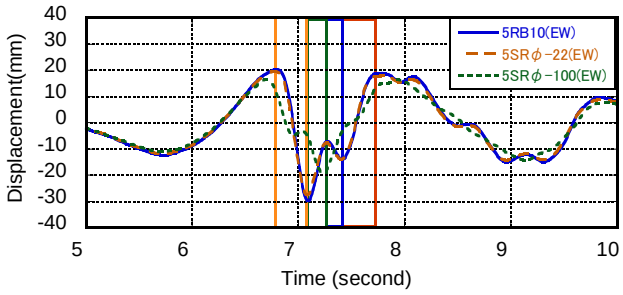

Fig.18(a) Displacement profile of soil beneath base-mat at No.5 reactor building

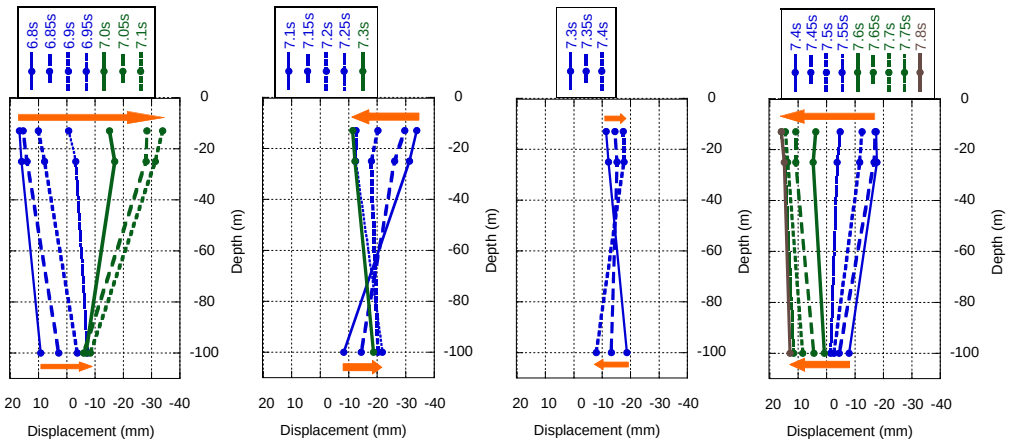

Fig.18(b) Deformation of soil beneath base-mat at No.5 reactor building

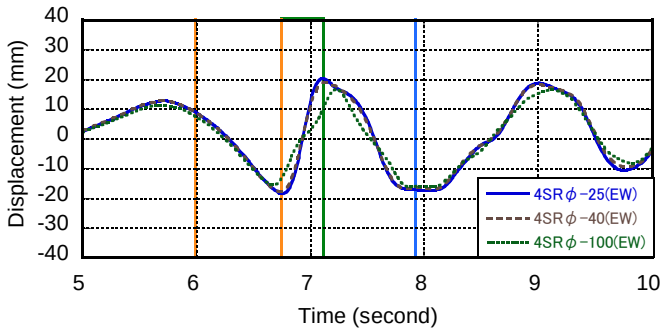

Fig.19(a) Displacement profile of soil beneath base-mat at No.4 reactor building

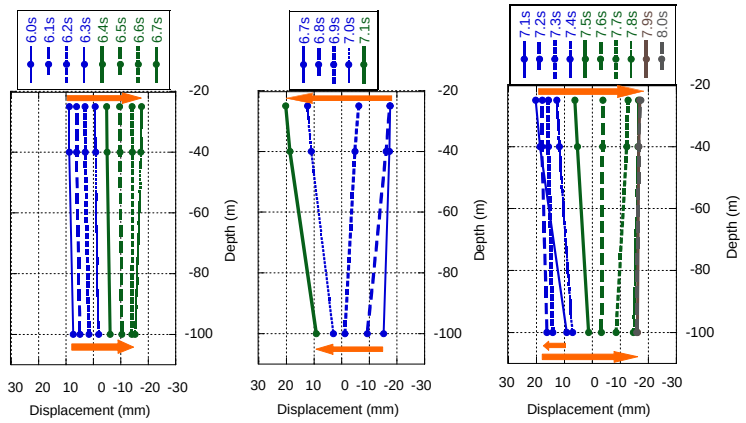

Fig.19(b) Deformation of soil beneath base-mat at No.4 reactor building

2.6 Identification of dual peaks in displacement profile by Ricker wavelets

By using the non-stationary Fourier spectra and the integrated displacement profile, it was derived that the maximum acceleration at the No.5 unit was caused by the local vibration mode in the surface soil from 22 to 100 meters.

The local vibration may be caused by a kind of plastic deformation, such as the crush and slip in the underground. The authors assumed that the gap between the foundation and its contacting soil caused the pulse wave and identified the pulse wave in the seismic record by the Ricker wavelet. This identification was also made in the seismic record at the Kashiwazaki-Kariwa NPS during Niigata-ken Chuetsu-oki earthquake in 2007 [3, 4].

Regarding the dual peaks at 5SRϕ-22 (EW) and the single peak at 5SRϕ-100 (EW), the authors identified them by superimposing the dual Ricker wavelets as shown Fig.20.

(1) The dual peaks are composed of the fundamental mode with 1.0Hz and the local mode with 3.0Hz judging from the non-stationary Fourier spectra (see Fig.20).

(2) The amplitude of the fundamental mode (1.0Hz) is set to 1.10 m/s^2 for 5SRϕ-22 (EW) and 0.5 m/s^2 for 5SRϕ-100 (EW). On the other hand, the amplitude of local mode (3.0Hz) is set to 3.0 m/s^2 for 5SRϕ-22 (EW) and 2.20 m/s^2 for 5SRϕ-100

(EW).

(3) Both wavelets are superimposed with an opposite sign in 5SRϕ-22 (EW) and with the same sign in 5SRϕ-100 (EW).

(4) To adjust to the displacement profile of the seismic record, both wavelets are superimposed with a delay of 0.04 seconds.

From the displacement profile of the identified Ricker wavelet, it may be concluded that the amplification at the No.5 unit was caused by the deformation with the amplitude 20mm in the surface soil.

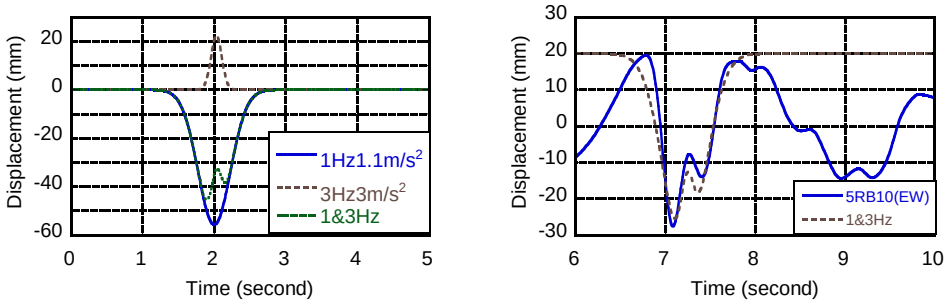

Identification of underground until 22 meters

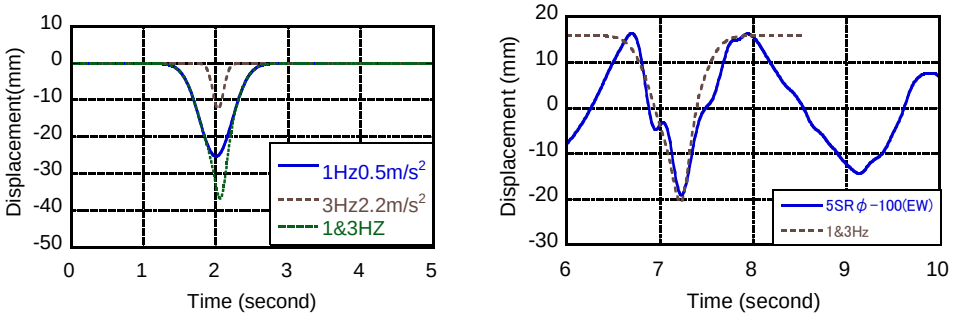

Identification of underground until 100 meters

Fig.20 Identification by dual Ricker wavelets

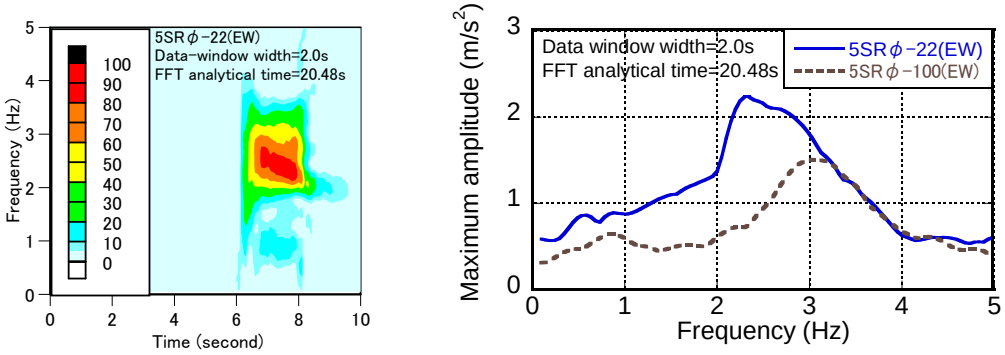

Fig.21 Non-stationary Fourier spectra and maximum amplitude spectra beneath the center of reactor building at No.5 unit (GL-22m)

2.7 Other possibilities of causes of frequency shift

Regarding the possibility of the topographic amplification of ground motion, Chubu Electric Power Co., Inc. detected the area of a low shear wave velocity in the underground from 200m to 400m. But it was found that the local mode occurred from the 5SRϕ-22 and 5SRϕ-100. This indicates that the nonlinearity should be considered in the narrow area.

The local site condition of underground was explained in terms of the shear wave velocity and the property of underground from 22m to 100m was considered uniform (see Fig.5). The offset vertical seismic profile (investigation at two boring sites) was investigation by Chubu Electric Power Co., Inc. after the Suruga Bay earthquake in 2009 and the uniform condition of underground at the No.5 unit was confirmed.

Furthermore, the detailed analysis of the records from the main-shock and after-shock at almost the same fault place revealed that, while the frequency shift was observed in the records from the main-shock, it was not in the records from the aftershock. This supports clearly that the frequency shift is attributed to the soil-nonlinearity for the average shear strain between SRϕ-22 and SRϕ-100.

The propagation of ground motion from the rupture area can also be excluded from the occurrence mechanism of amplification from the view point of the distance. The distance (0.4km) from the No.5 unit to the No.4 unit is extremely shorter than the distance (40km) from the No.5 unit to the epicenter. The effect of the fault rupture should be considered equally in the No.4 unit and the No.5 unit.

3. Rocking mode of foundation and induced local vertical mode

Recently the seismic design force is being re-estimated by investigating the seismic records with the large acceleration value [16]. The uplift of the foundation is one of the critical issues in the seismic design [1, 20-22]. At the Hamaoka NPS, several seismometers were arranged on the foundation. Using the seismic records, the authors aim to make clear the seismic behaviors of the foundation. Several factors affecting the uplift of foundations are illustrated in Fig.22.

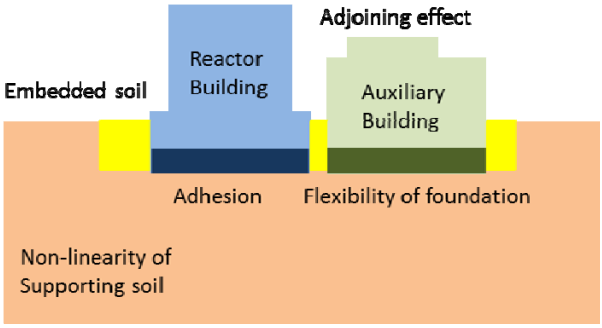

Fig. 22 Factors affecting uplift of foundation [1]

3.1 Seismic behavior of foundation at reactor building (No.5 unit)

As for the EW component, the acceleration and displacement profiles at 5RB2 (north-center position) and 5RB13 (south-center position) are almost coincident. This results from the uniform displacement of the rigid foundation. On the other hand, as for the UD component, the acceleration and displacement profiles at 5RB3 (north-east position) and 5RB14 (south-east position) are different in the phase and the amplitude. As shown in Fig.23, the duration of one cycle at the displacement profile of 5RB14 (UD) (0.37 seconds; 2.7Hz) is longer than that at 5RB3 (UD) (0.34 seconds; 2.9Hz). The acceleration amplitude at 5RB14 (UD) is two times larger than that at 5RB3 (UD).

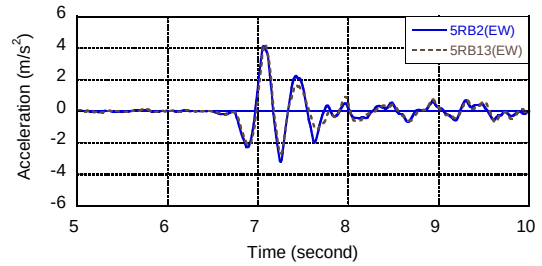

Acceleration profile (EW)

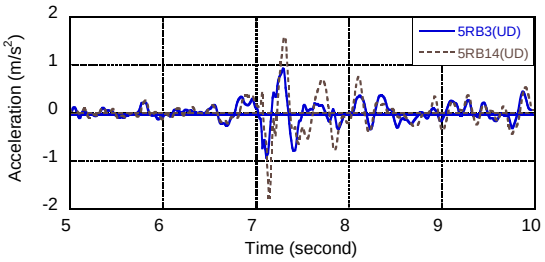

Acceleration profile (UD)

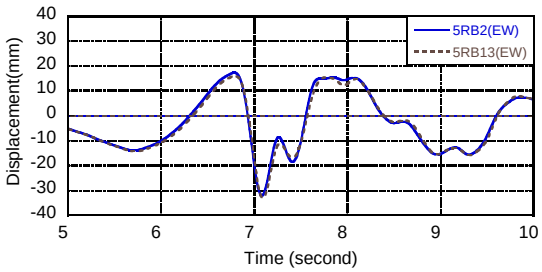

Displacement profile (EW)

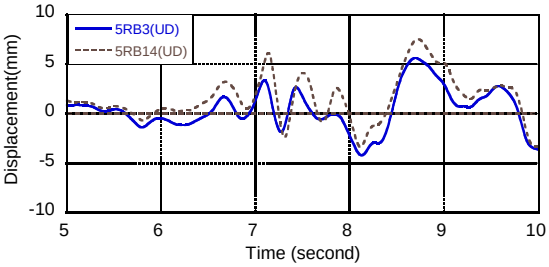

Displacement profile (UD)

Fig.23 Acceleration and displacement profiles (No.5 unit)

Comparing the non-stationary Fourier spectra at 5RB3 (UD) and 5RB14 (UD) (see Fig.24), the frequency components at 5RB14 (UD) are scattered in the frequency range higher than 7Hz. From the maximum amplitude spectra, it was detected that the maximum acceleration 0.98m/s^2 at RB14 (UD) is larger than 0.62m/s^2 at RB3 (UD).

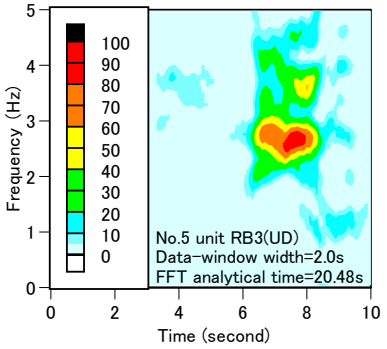

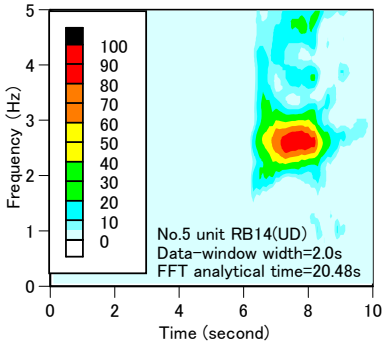

5RB3(UD) North-position　　5RB14(UD) South-position

Non-stationary Fourier spectra

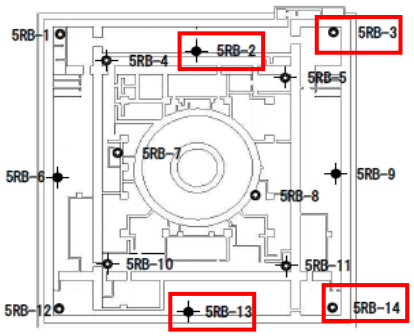

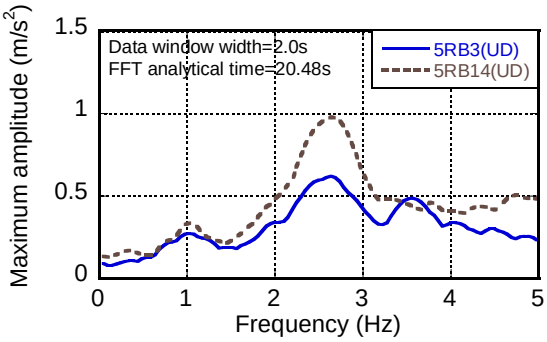

Maximum amplitude spectra

Fig.24 UD component on foundation at reactor building (No.5 unit)

3.2 Rocking mode of foundation at No.4 unit and No.5 unit

The maximum accelerations are listed in Table.2. The maximum accelerations at the No.5 unit are about two times larger than that at the No.4 unit. In the acceleration profiles, the main shock occurred at 7 seconds with the duration of 2 seconds. In the displacement profiles, the maximum peak-to-peak displacement at the No.4 unit occurred after 10 seconds and that at the No.5 unit occurred after 8 seconds.

The shapes of four displacement profiles are different during the main shock. On the other hand, the profiles after the main shock are coincident each other, which indicates the uniform deformation of foundation (see Fig.25).

Table 2 Maximum values of vertical acceleration on foundation (m/s^2)

4RB1	4RB3	4RB10	4RB12	5RB1	5RB3	5RB12	5RB14
76.71	52.71	55.29	45.21	149.79	94.44	95.27	176.95

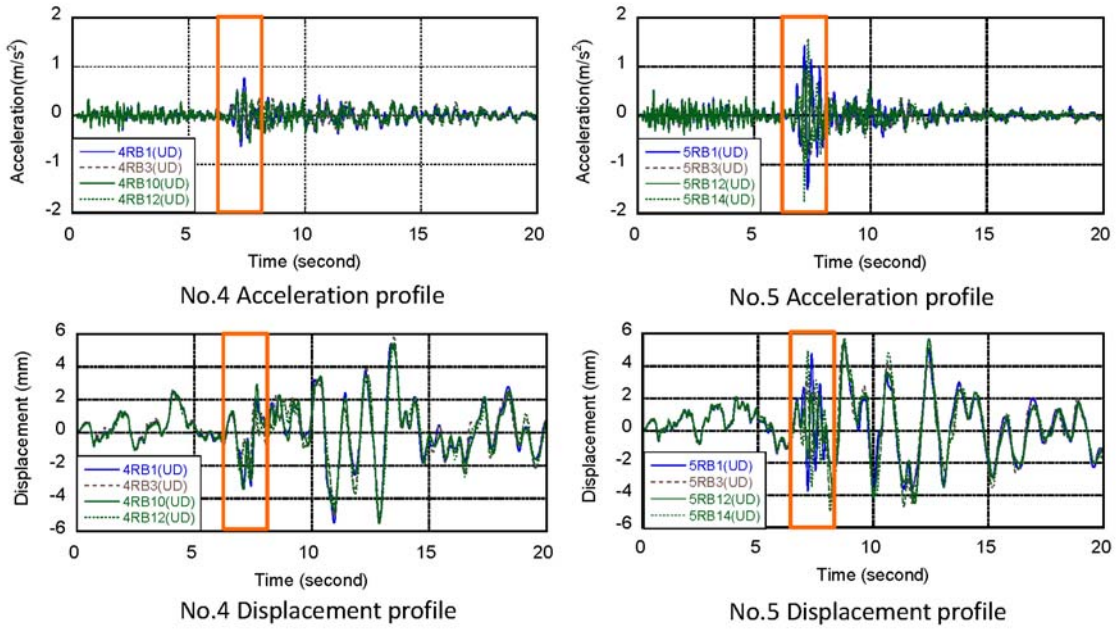

Fig.25 Comparison of acceleration and displacement profiles (No.4 and No.5 units)

Focusing on the displacement profile during the main shock from 6 to 8 seconds (see Fig.26), three deformation states of the foundation are illustrated with the interval of 0.05 seconds in Fig.27.

(1) North side (4RB1 and 4RB3, 5RB1 and 5RB3)

(2) South side (4RB10 and 4RB12, 5RB12 and 5RB14)

(3) Diagonal direction (4RB3 and 4RB10, 5RB1 and 5RB14)

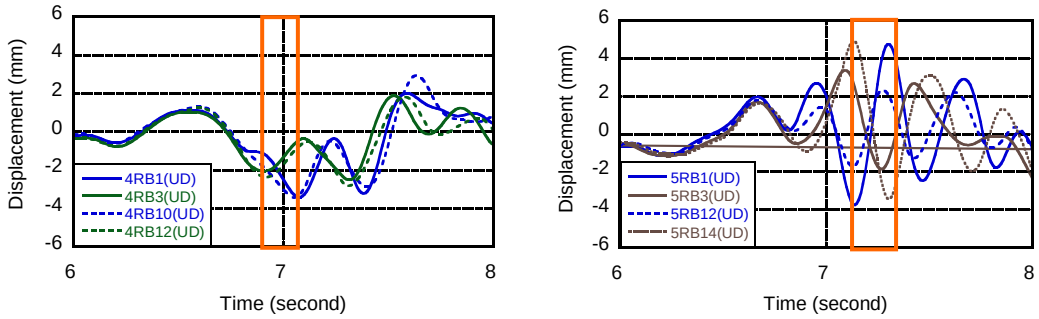

No.4 unit No.5 unit

Fig. 26 Displacement profile at foundation

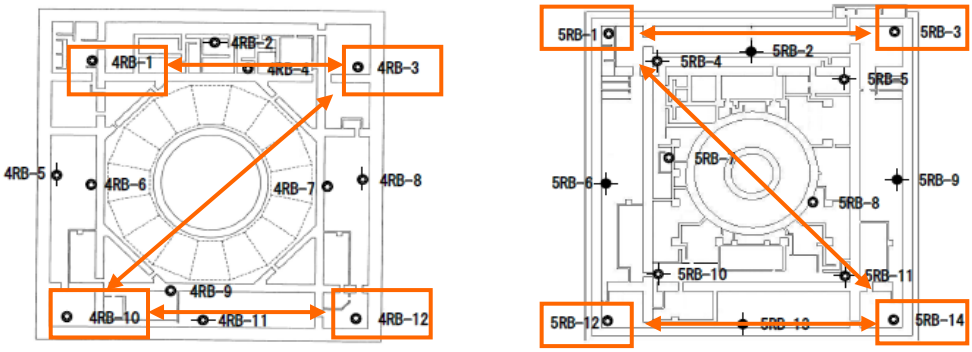

Fig.27 Illustrative direction of deformation at foundation

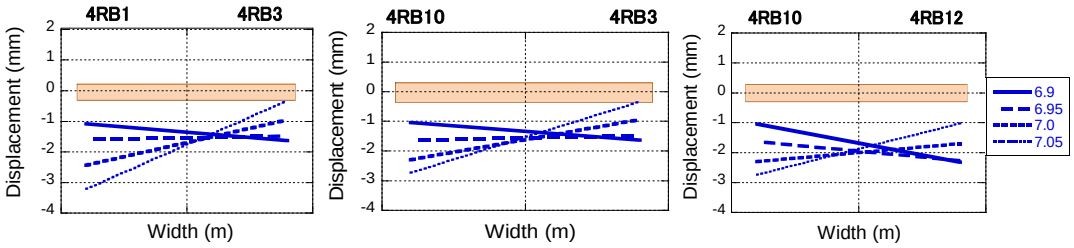

Deformation of No.4 unit foundation

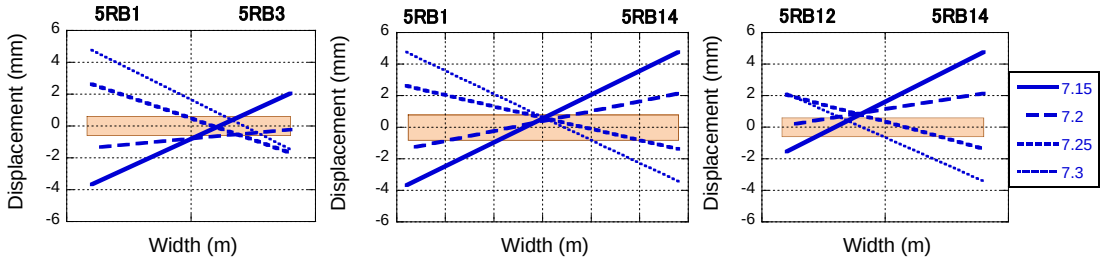

Deformation state of No.5 unit foundation

Fig.28 Rocking mode of foundation

As shown in Fig.28, the deformation of the No.4 unit from 6.9 to 7.05 seconds shows the rocking vibration. Its amplitude is about 2mm and the center of rocking is almost at the center of the foundation. The deformation state of the No.5 unit from 7.15 to 7.3 seconds shows also the rocking vibration, the amplitude of which is about 9mm. At the reversal point, the deformation of the foundation is illustrated as an isometric figure in Fig.29.

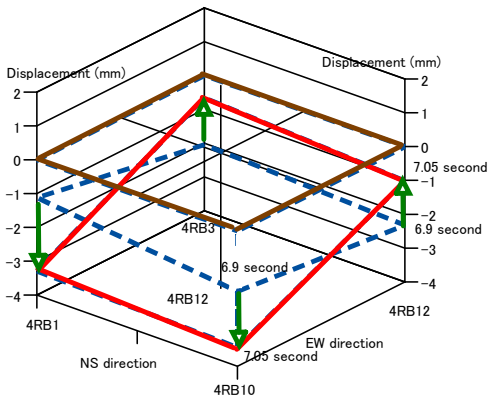

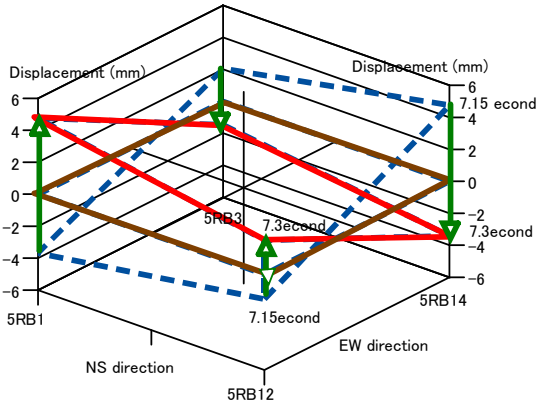

No.4 unit　　No.5 unit

Fig. 29 Deformation of foundation

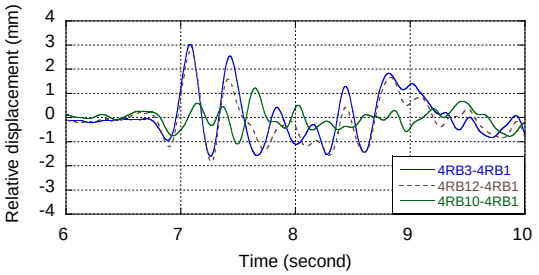

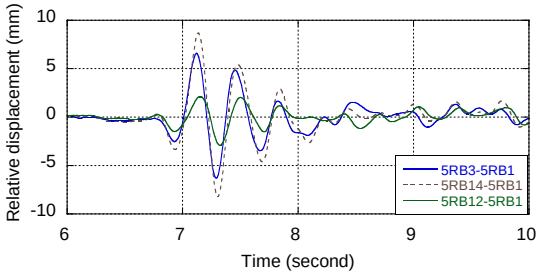

No.4 unit　　No.5 unit

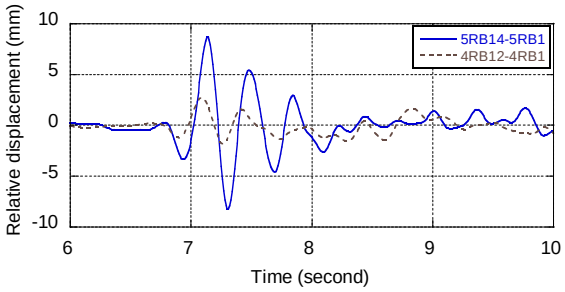

Comparison between No.4 unit and No.5 unit

Fig.30 Relative displacement at foundation

To make clear the rocking mode of the foundation, the relative displacement from RB1 is calculated such as $\overline{X}_{RB1}^{RB3}(t) = X_{RB3}(t) - X_{RB1}(t)$, which is illustrated in Fig.30.

The rocking mode of foundation can be explained as follows.

(1) The profiles of $\overline{X}_{4RB1}^{4RB3}(t)$ and $\overline{X}_{4RB1}^{4RB12}(t)$ are almost coincident.

(2) The amplitude of $\overline{X}_{4RB1}^{4RB10}(t)$ is smaller than that of $\overline{X}_{4RB1}^{4RB3}(t)$ and $\overline{X}_{4RB1}^{4RB12}(t)$.

(3) The rocking mode of the No.4 unit occurred in the east-west direction.

(4) The rocking mode of the No.5 unit occurred in three cycles from 6 to 8 seconds.

(5) The relative displacement profile of $\overline{X}_{5RB1}^{5RB14}(t)$ is larger than those of $\overline{X}_{5RB1}^{5RB3}(t)$ and $\overline{X}_{5RB1}^{5RB12}(t)$

(6) The axis of the rocking mode is in the direction of north-east and south-west.

(7) The maximum amplitude of $\overline{X}_{5RB1}^{5RB14}(t)$ is three times larger than that of $\overline{X}_{4RB1}^{4RB12}(t)$.

3.3 Vertical acceleration induced by uplift of foundation

In Fig.31, the vertical acceleration profiles at 5RB1 (UD), 5RB3 (UD), 5RB12 (UD) and 5RB14 (UD) are illustrated, in which the acceleration profile at 5RB14 (UD) includes a higher mode from 7 to 7.3 seconds. To make clear the occurrence mechanism of the higher mode, the acceleration profile is illustrated together with the displacement profiles at four corners (see Fig.32).

The higher mode at 5RB14 (UD) occurs when the displacement profile at 5RB3 (UD) approaches the zero displacement. This higher mode is considered as the vertical acceleration induced when the uplifted foundation contacts to the soil.

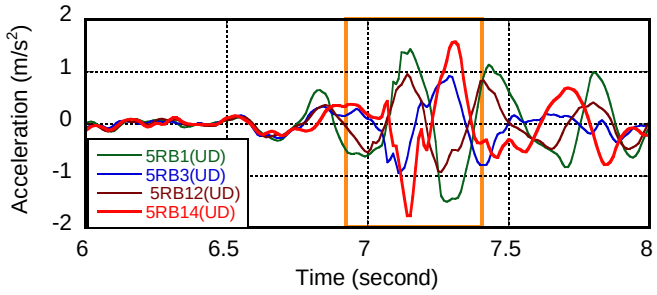

Fig.31 Acceleration profiles at four corners of foundation

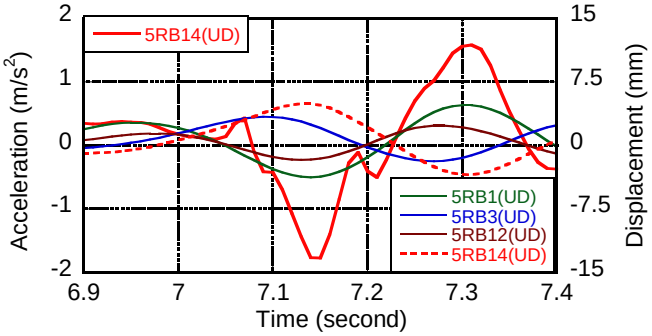

Fig.32 Acceleration induced by uplift of foundation

The induced vibration mode at 5RB14(UD) is evaluated by the non-stationary Fourier spectra, in which the frequencies of additional modes are scattered in the frequency range higher than 4Hz with an amplitude 0.50m/s^2 (see Fig.33).

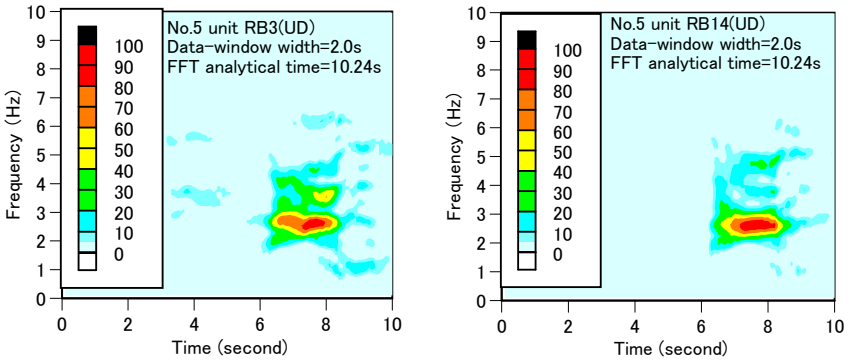

5RB3 (UD): north-east　　5RB14 (UD): south-east

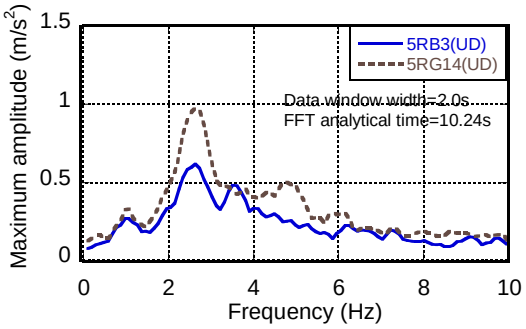

Fig.33 Induced higher mode by rocking of foundation
(Non-stationary Fourier spectra and maximum amplitude spectra)

3.4 Orbit of displacement

Consider the three-component displacement time histories at SRϕ-22 (underground 22m) and SRϕ-100 (underground 100m) as shown in Fig.34. Fig.35 shows the orbit of displacement from 6.65 to 7.65 seconds in Fig.34 to evaluate the seismic behavior including the vertical ground motion. Three combinations of the NS, EW and UD components are considered. In the orbit of the EW and the UD component at SRϕ-22, the vertical displacement with the amplitude 20mm occurred at both reversal points of the EW displacement. The displacement of the NS component changed the direction of movement in the process of decreasing displacement of the EW component. These behaviors may result from the uplift of foundation.

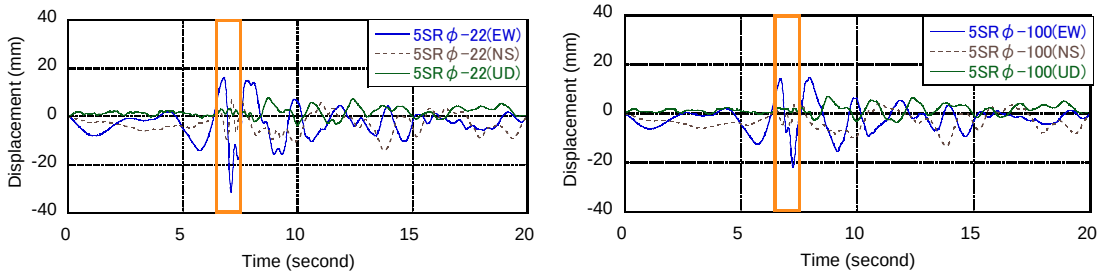

Fig.34 Displacement time histories

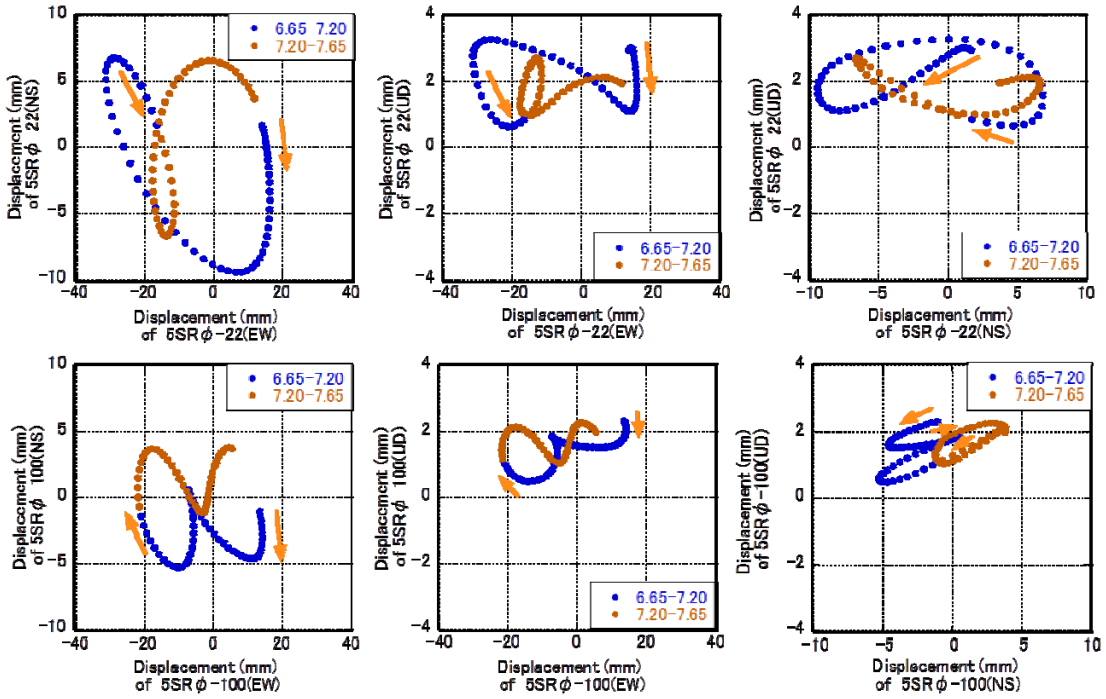

Fig.35 Orbit of displacement

3.5 Simplified model

The authors have conducted the analytical research using the information on the seismic records. From the analytical results and site investigation after the Niigata-ken Chuetsu-oki earthquake in 2007, the interaction between the building and the surrounding soil was considered to be caused by the non-linearity in the surrounding soil. In addition, the authors investigated the seismic behavior by using a simplified model with various nonlinear hysteresis rules (see Fig.36 and Fig.37).

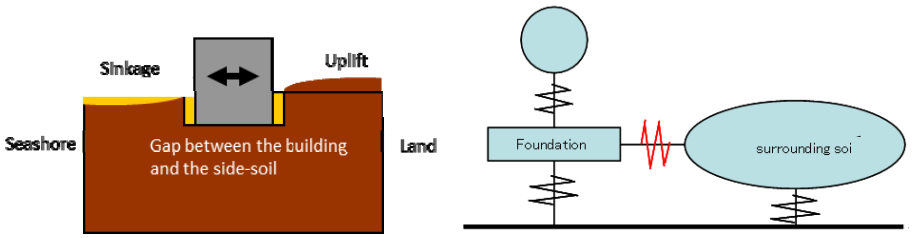

Fig.36 Gap model and simplified model

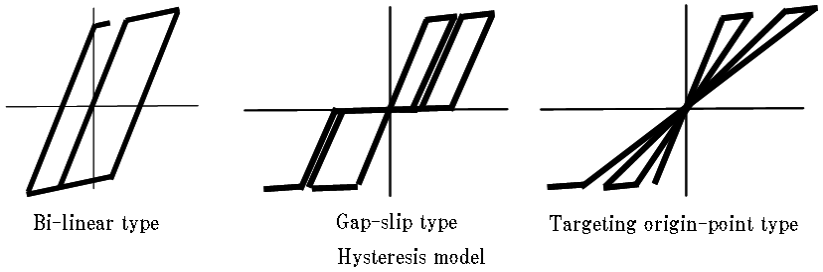

Fig.37 Different hysteresis models of element between building and surrounding soil

Fig.38 shows examples of the analytical results for these different hysteresis models of the element between a building and surrounding soil.

The Ricker wavelet (2.0Hz) of various levels was input and it was found that the maximum response of the Gap-slip model was the largest (see Fig.39).

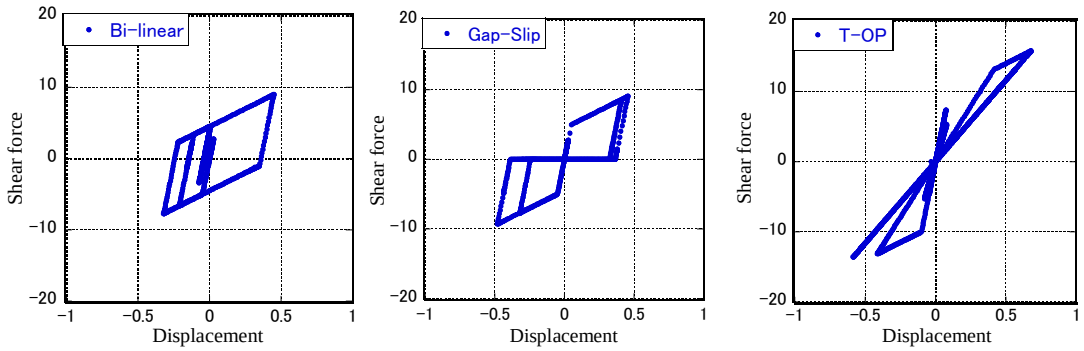

Fig.38 Examples of analytical results for different hysteresis models of element between building and surrounding soil

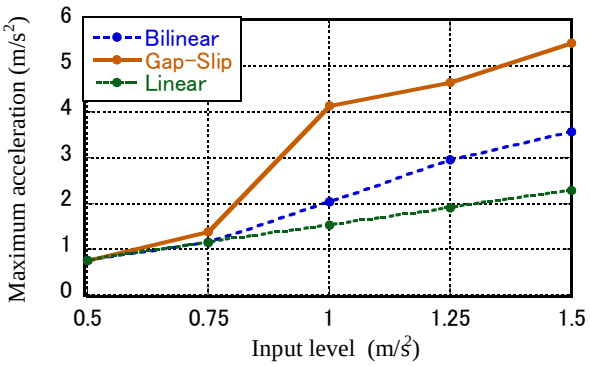

Fig.39 Maximum acceleration for increased level of Ricker wavelet

Recent earthquake events in Japan provided us with many seismic records. Especially the seismic records measured at the nuclear power plants through the high

density-array system were precious database. It is expected that those information enables the refinement of the analytical models.

4. Discussions and conclusions

The interaction between a building and its surrounding soil is one of the main subjects in the seismic design of the nuclear power plants (for example [23, 24]). The damping effect by the surrounding soil has been one of the important subjects (for example [25, 26]). The small amount of seismic data has disturbed the further refinement of the seismic design of such structures.

The seismic records at the Hamaoka NPS during the Suruga Bay earthquake in 2009 included the records in the underground and provided us with useful information on the design of nuclear power stations. Using the non-stationary Fourier spectra and the numerically integrated displacement profiles of the seismic records, the occurrence mechanisms of the large acceleration 4.38m/s^2 were investigated in detail. The rocking mode of the foundation and the induced acceleration by the uplift of the foundation were also discussed. The following findings have been obtained.

(1) The deformation profile in the depth direction has been illustrated in the interval of 0.05 seconds. The opposite-direction movement between 22-100 meters in the underground is related to the maximum acceleration.
(2) The amplification observed at the No.5 unit did not occur in the No. 4 unit.
(3) The maximum acceleration 4.38m/s^2 at 5RB10 (EW) may be induced by the local vibration mode in the ground 22-100 meters below the ground surface.
(4) The consideration of local vibration modes is necessary for more reliable design of nuclear power plants.
(5) The shape of the dual peaks in the displacement profile has been identified by imposing dual Ricker wavelets. The dominant frequencies and amplitudes have been estimated from the non-stationary Fourier spectra.
(6) In the underground 22-100 meters below the reactor building, the frequency of the dominant component shifted from 3.0Hz to 2.5Hz in the time from 6 to 8 seconds. This indicates the deterioration of the soil stiffness.
(7) The average strain in the underground from 22 meters to 100 meters was calculated using the displacement. The reduction ratio of shear stiffness was estimated to be 30 percent.
(8) From the vertical displacement at the four corners of the foundation, the rocking vibration mode has been detected.
(9) The amplitude of the rocking mode at the No.5 unit is three times larger than that

at the No.4 unit. The rocking mode is considered to be related to the deformation of underground. The possibility of the existence of rocking vibration should be investigated for more reliable design of nuclear power plants.

(10) In the record at 5RB14 (south-east), the higher mode induced by the uplift of the foundation has been detected.

Acknowledgements

The seismic records including those in the underground were provided by the Chubu Electric Power Company Co., Inc. and K-NET. We deeply appreciate the Chubu Electric Power Company Co., Inc. and National Research Institute for Earth Science and Disaster Prevention.

References

[1] Japan Nuclear Energy Safety Organization (JNES) (2008) "Test of soil and structure non-linear interaction at nuclear power facility and analytical research on the seismic behavior of building foundation in revision work of standard" *JNES/SSD08-022* October 2008 (in Japanese), (Available from <http://www.jnes.go.jp/content/000004810.pdf> {Accessed on January 30th 2013}).

[2] Japan Nuclear Energy Safety Organization (JNES) (2009) "Analysis of seismic behavior of building foundation by seismic records" *JNES/SSD09-004* March 2009 (in Japanese), (Available from <http://www.jnes.go.jp/content/000016346.pdf> {Accessed on January 30th 2013}).

[3] Kamagata, S. (2009) "Non-stationary property of Niigata-ken Chuetsu-oki Earthquake on Kashiwazaki-Kariwa nuclear power plants (Occurrence mechanism of pulse-like wave)", *Annual meeting of Architectural Institute of Japan*, 1007-1008 (in Japanese).

[4] Kamagata, S. Takewaki, I (2013). "Occurrence mechanism of recent large earthquake ground motion at nuclear power plant sites in Japan under soil-structure interaction", *Earthquakes and Structures*, 4(5), 557-585.

[5] National Research Institute for Earth Science and Disaster Prevention (NIED) (2009b), "Peak Acceleration Contour Map 2009/0/11-05:0734.785N 138.498E 23km M6.5", (Available from <http://www.kyoshin.bosai.go.jp/kyoshin/share/index_ multi.html> {Accessed on January 30th 2013}).

[6] Nuclear and Industrial Safety Agency (NISA) (2010a). "Abstract of Application of permission for the establishment as to the change and alteration of No.1, No.2, No.3, No.4 and No.5 unit of nuclear reactor building facilities at Hamaoka nuclear power station of Chubu Electric Power Company" , (Available from <http://www.aec.

go.jp/jicst/NC/iinkai/teirei/siryo2010/siryo59/siryo4-2.pdf> {Accessed on January 30th 2013}).

[7] Chubu Electric Power Company (2009). ‘‘Acceleration time history data of the Suruga-gulf earthquake in August 11th 2009 (Main-shock and After-shock)’’, distributed by Japan Association for Earthquake Engineering.

[8] Chubu Electric Power Company (2010a). ‘‘State of Hamaoka nuclear power station regarding to the Suruga-gulf earthquake’’, *Public announcement,* November 23rd 2010 (in Japanese), (Available from http://www.pref.shizuoka.jp/bousai/event/documents/siryou2-2.pdf {Accessed on January 30th 2013})).

[9] Chubu Electric Power Company (2010b). ‘‘Conformation on seismic safety of No.5 unit of Hamaoka nuclear power station regarding to the Suruga-gulf earthquake in 2009’’, *Public announcement,* December 3rd 2010 (in Japanese), (Available from http://www.meti.go.jp/committee/summary/0004450/060_s02_01.pdf {Accessed on January 30th 2013}).

[10] Chubu Electric Power Company (2012a). ‘‘Conformation on seismic safety of No.5 unit of Hamaoka nuclear power station regarding to the Suruga-gulf earthquake in 2009’’, *Public announcement,* January 7th 2012 (in Japanese), (Available from <http://www.pref.shizuoka.jp/bousai/event/documents/siryou1-1.pdf> {accessed on January 30th 2013}).

[11] Chubu Electric Power Company (2012b). ‘‘Report on soundness of Hamaoka nuclear power station No.5 by seismic response analysis unit during Suruga Bay earthquake on 2009”, *Public announcement,* October 2010 (in Japanese), (Available from<http://www.nsr.go.jp/archive/nisa/oshirase/2009/files/211002-8-1.pdf> {Accessed on January 30th 2013}).

[12] Matsumoto, J (2010) “Ground motion characteristics at Hamaoka Nuclear Plant during Suruga Bay Earthquake of August 11, 2009” *No.21352, 703-704, Annual meeting of Architectural Institute of Japan* (in Japanese).

[13] Japan Association for Earthquake Engineering (2013). “Strong Earthquake Records”, (Available from <http://www.jaee.gr.jp/jp/stack/data/ >{Accessed on January 30th 2013}).

[14] National Research Institute for Earth Science and Disaster Prevention (NIED 2009a) “Strong-motion Seismograph Networks (K-NET, Kik-net)”, (Available from <http://www.kyoshin.bosai.go.jp/> {Accessed on January 30th 2013}).

[15] Kamae, K., Kawabe, H. and Irikura, K. (2004). ‘‘Strong ground motion prediction for huge seduction earthquake using characterized source model and several simulation techniques’’, *Proc. of the 13th WCEE,* Vancouver.

[16] Strasser, F.O. and Bommer, J.J. (2009). Large-amplitude ground-motion recordings and their interpretations, *Soil Dynamics and Earthquake Engineering*, 29, 1305–1329.

[17] Ohmachi, T. Inoue, S. Mizuno, K. and Yamada, M. (2011). "Estimated cause of extreme acceleration records at the KiK-net IWTH25 station during the 2008 Iwate-Miyagi Nairiku earthquake, Japan" *Transactions of Japan Association for Earthquake Engineering*, 11(1), 32-47(in Japanese).

[18] Kamagata, S. (1991). "Non-stationary spectra for seismic response control", *News & Topics Research & Development Structural Engineering (KRCEE0019111501)*, Kobori Research Complex (in Japanese).

[19] Nuclear and Industrial Safety Agency (NISA) (2010b) "Adjustment of deliberation on factor of amplification in seismic record of Hamaoka nuclear power station No.5 unit on Suruga-gulf earthquake in 2009" *Public announcement*, December 15th 2010 (in Japanese), (Available from <http://www.nsr.go.jp/archive/nisa/shingikai/107/files/221215-1.pdf> {Accessed on January 30th 2013}).

[20] Miyamoto, A., Tomura, H., Yamamoto, M and Ogata, R. (1988). "Relation between site condition and induced vertical motion due to base mat uplift of nuclear plants" *Annual meeting of Architectural Institute of Japan*, 1169-1170 (in Japanese).

[21] Nakamura. N, Ino, S. Kurimoto, O. and Miake, M. (2007) "An estimation method for basemat uplift behavior of nuclear power plant buildings" *Nuclear Engineering and Design*, 237, 1275-1287.

[22] Gazetas, G. , Anastasopoulos,I., Adamidis,O. and Kontoroupi, Th. (2013). Nonlinear rocking stiffness of foundations, *Soil Dynamics and Earthquake Engineering* (in press).

[23] Tajimi, H. (1984) "Recent tendency of the practice of soil-structure interaction design analysis in Japan and its theoretical background" *Nuclear Engineering and Design*, 80, 217-231.

[24] Bolisetti, C. and Whittaker, A.S. (2011). Seismic structure-soil-structure interaction in nuclear power plant structures, *Transactions*, SMiRT 21, 6-11 November, 2011, New Delhi, India.

[25] Muto, K. Omatsuzawa, K (1972) "Earthquake response analysis for a BWR nuclear power plant using recorded data", *Nuclear Engineering and Design*, 20, 385-392.

[26] Akino, K. and Tajimi, H. (1965). "Aseismic design and dynamic analysis of nuclear Power plants: Part II Rocking motion, Swaying motion" *Nuclear Structural Engineering*, 2(1), 120-125.

Appendix-1 Numerical integration of acceleration record

The drift of the seismic records is inevitable in the numerical integration as shown in Fig.A1-1. The solid line is the integrated displacement with band-pass filter and the dotted line is the integrated displacement without band-pass filter. In this paper the local vibration mode is targeted with the frequency range from 0.5Hz to 20Hz. The trapezoidal band-pass filter in frequency range is adopted as shown in Fig.A1-2. Furthermore the average-zero compensation in the integrated velocity profile is adopted. The average velocity over the duration is defined by $V_{AV} = \sum_{i=1}^{N} V(i) / N$ and the zero-line compensation by average velocity is computed by $V(t) = V(t) - V_{AV}$. The effect of the compensation with the average velocity is shown in Fig.A1-3.

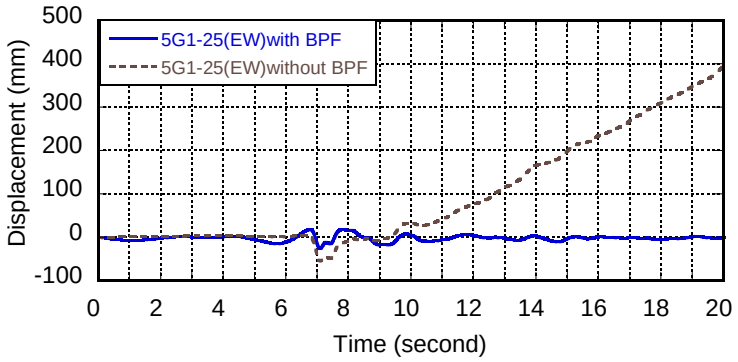

Fig.A1-1 Drift phenomenon in integrated displacement profile

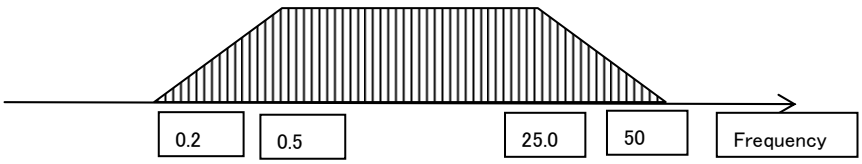

Fig.A1-2 Band-pass filter

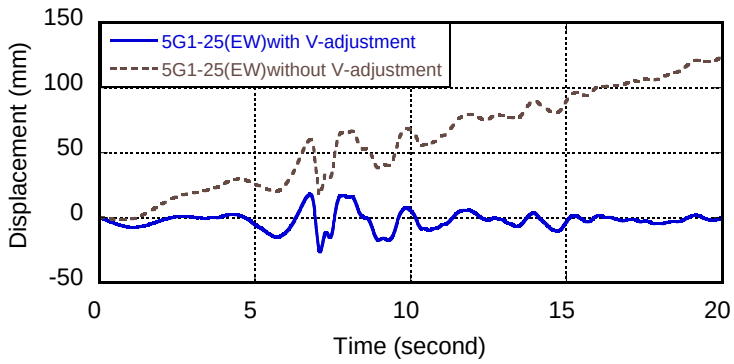

Fig.A1-3 Effect of adjustment by average velocity

The zero line correction by the average of velocity is influenced by the length of records. As to the seismic record at 5RB-3(UD), the displacement profiles of three kinds of data length are compared in Fig.A1-4. The displacement profile of the data length (2000 steps) shows a drift in the negative direction. The displacement profiles of the data length (4000 steps and 6000 steps) are almost coincident each other.

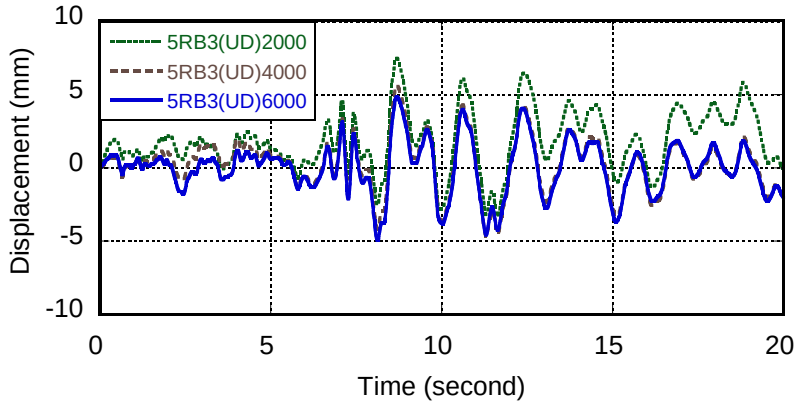

Fig.A1-4 Effect of data length

Regarding to the seismic record at the No.4 unit, the displacement profiles of the data length (4000 steps) are compared as shown in Fig.A1-5. At the No.4 unit, four displacement profiles at the corner of foundation are almost coincident each other (see Fig.A1-5).

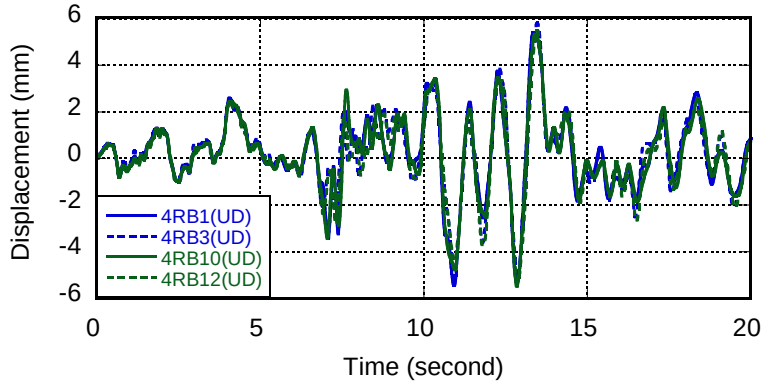

Fig.A1-5 Displacement profile at No.4 unit

Appendix-2　Ground motion property in neighboring area of Hamaoka NPS

To evaluate the locality of amplification at the No.5 unit, the seismic records at the Hamaoka area neighboring the Hamaoka NPS are analyzed using the seismic records of K-NET. The non-stationary Fourier spectra at 1RB1 and K-NET (Hamaoka) are compared (see Fig.A2-1 and Fig.A2-2). The dominant components at 1RB1 (EW) are almost coincident with the dominant components at Hamaoka (EW). As to NS and UD components, the dominant components at K-NET (Hamaoka) include many frequency components in the frequency range lower than 6Hz.

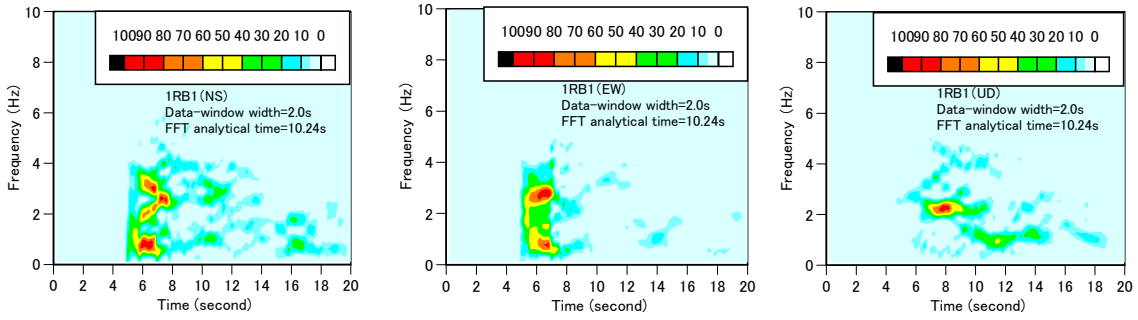

No.1 unit foundation of reactor building

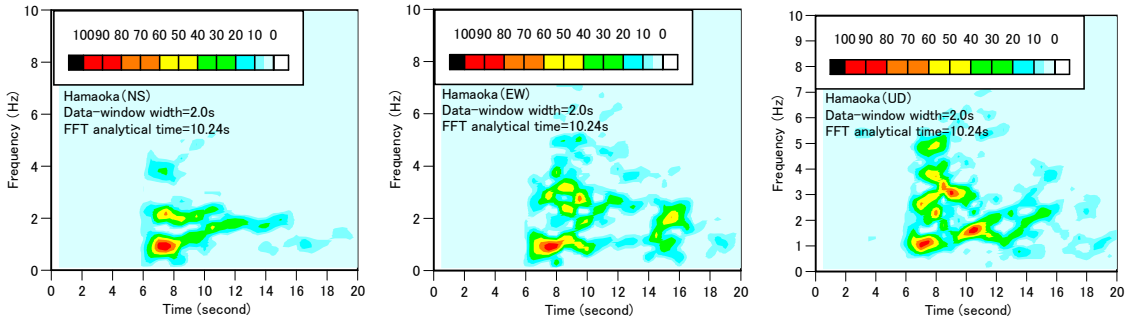

K-NET (Hamaoka)

NS component　　EW component　　UD component

Fig.A2-1 Non-stationary Fourier spectra at 1RB10 and K-NET (Hamaoka)

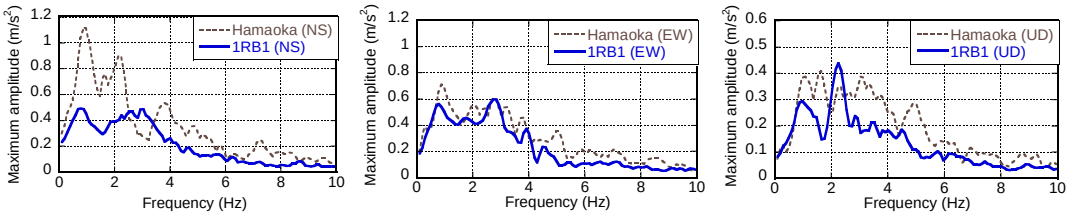

NS component　　EW component　　UD component

Fig.A2-2 Comparison of maximum amplitude spectra at K-NET (Hamaoka) and 1RB1

The seismic record at 5RB10 is compared with that from K-NET (Haibara) to evaluate the singularity of the maximum value (4.38m/s^2). The dominant components at Haibara are scattered in the frequency range lower than 6Hz. The large amplification at Haibara may result from the shorter distance from the epicenter. However the dominant component at 2.5Hz is observed in both seismic records. Judging from this observation, the maximum value at 5RB10 (EW) may not be singular in the neighboring area of Hamaoka NPS.

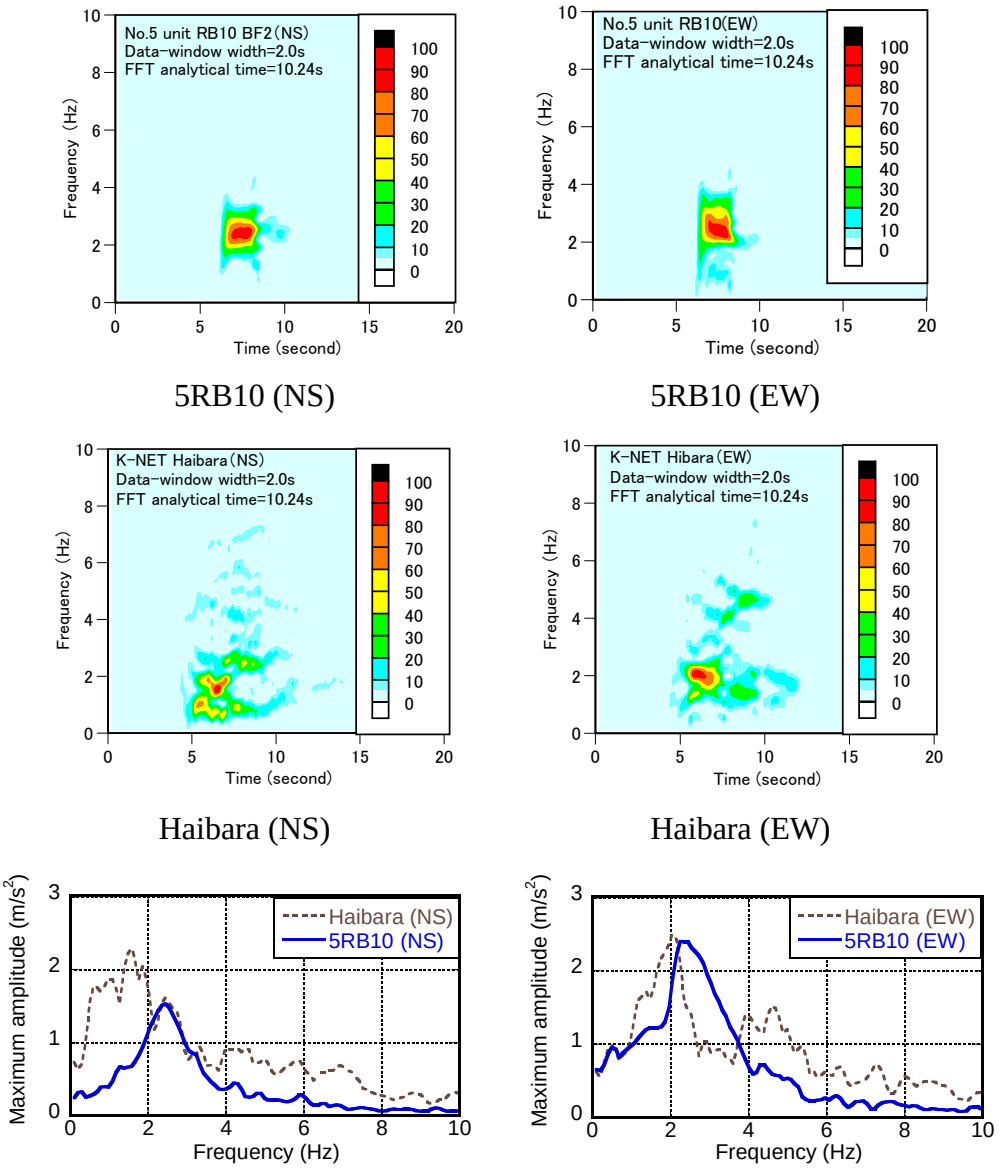

Fig.A2-3 Comparison of non-stationary Fourier spectra and maximum amplitude spectra at K-NET (Haibara) and 5RB10